COMMUNICATION

ADVANCED MATERIALS

DOI: 10.1002/adma.200702712

Hierarchically Organized Carbon Nanotube Arrays from Self-Assembled Block Copolymer Nanotemplates**

By *Duck Hyun Lee, Dong Ok Shin, Won Jong Lee,** and *Sang Ouk Kim**

The ideal 1D structure of carbon nanotubes (CNTs) lends them various attractive properties such as tunable conductivity, extremely high electron mobility, and large charge storage capacity.[1,2] Owing to their molecular scale dimensions and unique electronic properties, CNTs are considered to be promising building blocks for future nanoelectronics devices, and are attractive candidates for overcoming the fundamental limitations of conventional Si-based microdevices.[3] CNTs need to be integrated within device architectures for nanoelectronics applications.[4,5] However, the development of a robust large-scale organization process for assembling CNTs remains a formidable challenge.

For applications such as field emission[6] and nanoelectronics,[7] it is necessary to grow vertically oriented CNTs having desired properties at predetermined locations.[5] Of the various synthetic approaches for growing CNTs, chemical vapor deposition (CVD), which is a facile and easily scalable process, is the most widely used method for the vertical growth of CNTs. In a typical CVD experiment, metal particles on a substrate surface catalyze the vertical growth of CNTs. As a consequence, the diameter and position of the obtained individual CNTs are determined by the size and lateral distribution of the catalyst particles.

Catalyst particles for the vertical growth of CNTs are generally prepared by the deposition and heat treatment of a thin metal catalyst film on a substrate.[8,9] The deposited film dewets to form catalyst nanoparticles upon the heat treatment process.[10–12] However, the prepared catalyst particles are usually polydisperse in size and randomly distributed over the substrate surface. The application of lithographic patterning processes may lead to a narrower size distribution and relatively uniform lateral distribution of catalyst particles, but the intrinsic resolution limit of conventional photolithography processes implies that it is impossible to controllably fabricate catalyst particles with the desired nanoscale dimensions.

In the present work, we have developed a novel approach to fabricate hierarchically organized vertical CNT arrays by combining plasma-enhanced CVD (PECVD) with self-assembled block copolymer nanotemplates. Block copolymers are ubiquitously used self-assembling polymeric material that provide access to a variety of periodic nanoscale morphologies with feature sizes ranging from 5 to 50 nm.[13–21] Unlike other nanopatterning techniques such as focused electron-beam lithography or scanning probe lithography, block copolymer assembly is a parallel patterning process, thereby enabling easy scale-up. In our approach, an asymmetric block copolymer, polystyrene-*block*-poly(methyl methacrylate) (PS-*b*-PMMA) has been used to form cylindrical nanostructures with center-to-center distances between neighboring cylinders of 72 and 34 nm. These cylindrical assemblies have been used as nanotemplates for the hierarchical organization of CNTs. The entire process is schematically illustrated in Figure 1. A thin block copolymer film has been initially self-assembled on a neutral silicon wafer substrate to form a nanoscale morphology consisting of perpendicular PMMA cylinders within a PS matrix.[22,23] Next, the cylinder cores have been selectively etched to produce polymeric nanotemplates with hexagonally packed cylindrical nanopores.[14] The masked deposition of a iron catalyst has been performed over the nanotemplate, and a subsequent lift-off process has been used to establish control over the size and lateral distribution of the catalyst particles. The size and nanoscale distribution of the catalyst particles have been defined by the pattern size of the nanotemplate, whereas their lateral distribution over large areas is controlled by the micrometer-scale patterns physically engraved in the metal mask. After catalyst deposition, heat treatment at 750 °C has been used to further reduce the size of the catalyst particles. Upon the subsequent PECVD growth of CNTs, the diameter and lateral distribution of the CNTs is determined by the size and location of the catalyst particles. The vertical alignment of the CNTs has been controlled by adjusting the strength of an applied electric field. The CNT growth process has been directed to produce a well-organized 3D hierarchical architecture. Since the overall process including nanotemplate self-assembly, catalyst deposition, and CNT growth entails parallel processing, this novel approach is readily scalable to macroscopic scales.

The left panel in Figure 2a shows a scanning electron microscopy (SEM) image of the as-deposited catalyst

[*] Prof. W. J. Lee, Prof. S. O. Kim, D. H. Lee, D. O. Shin
Department of Materials Science and Engineering
Korea Advanced Institute of Science and Technology (KAIST)
Daejeon 305-701 (Korea)
E-mail: wjlee@kaist.ac.kr; sangouk.kim@kaist.ac.kr

[**] This work was supported by the Center for Electronic Packaging Materials (ERC) of MOST/KOSEF (R11-2000-085-08 004-0), the second stage of the Brain Korea 21 Project, the Korea Government (MOEHRD) (KRF-2005-003-D00 085), the Korea Science & Engineering Foundation (R01-2005-000-10 456-0), the Korean Ministry of Science and Technology, and the Fundamental R&D Program for Core Technology of Materials funded by the Ministry of Commerce, Industry, and Energy, Republic of Korea.

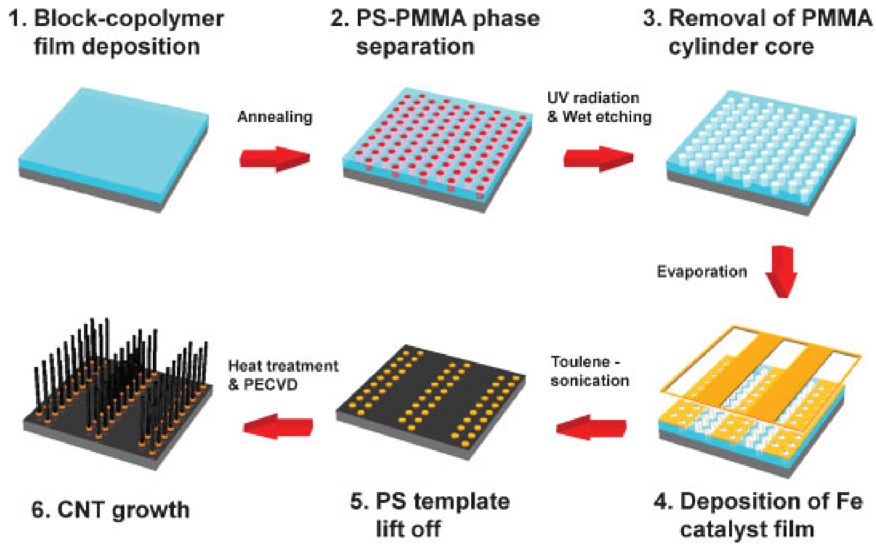

Figure 1. Schematic depiction of the hierarchical organization process used to fabricate vertical CNT arrays. A block copolymer thin film has been self-assembled onto a substrate, giving rise to hexagonally packed cylinders perpendicular to the surface. The cylinder cores have been selectively etched to form a nanoporous PS template. Selective deposition of the catalyst over the nanotemplate through a metal mask, followed by a lift-off step yields monodisperse catalyst nanoparticles hierarchically patterned at multiple length scales. Heat treatment of the catalyst particles and subsequent PECVD growth of CNTs from laterally patterned catalyst particles leads to the formation of highly oriented hierarchical CNT arrays.

nanoparticles. The catalyst particles have been selectively deposited through the nanopores of the block copolymer templates such that the hexagonal arrangement of the catalyst particles exactly duplicates the nanoscale morphology of the template. The right panel in Figure 2a shows a SEM image of the nanoparticles after heat treatment. Heat treatment at 750 °C for 1 min reduces the size of the catalyst particles from 21 to 14 nm. The diameter of CNTs grown on the catalyst nanoparticles is approximately half of the agglomerated catalyst particle size (Fig. 2b). Since the catalyst particles are extremely monodisperse in size, the CNTs grown from these catalysts are also very uniform. Figure 2c–h shows low-magnification views of hierarchically organized CNT arrays prepared by employing parallel, square, and hexagonal grid masks. Further variation of the shape of the deposition mask is likely to yield CNT arrays with non-regular shaped structures, which may potentially be useful for the device integration of vertical CNTs.

The diameter of CNTs grown by the CVD method is closely related to the size of the catalyst particles. In our approach, the size of the as-deposited catalyst particles is identical to the nanopore size in the block copolymer template. The nanopore size (D) and center-to-center distance between neighboring nanopores (L) of the block copolymer template depend on the molecular weight of the block copolymer (M), which is given by the following scaling law:

$$D,\ L \,\alpha\, M^{\frac{2}{3}} \qquad (1)$$

Thus, adjusting the molecular weight of the block copolymer leads to variations in both D and L (aerial density of nanopores). Further control over the catalyst size has been achieved by adjusting the amount of deposited catalyst film and by varying the heat-treatment protocol. This enables tuning of the catalyst size without influencing the distance between neighboring catalyst particles (aerial density of catalyst particles). Figure 3 present a series of SEM images of catalytic nanoparticles, as well as transmission electron microscopy (TEM) images of the corresponding CNTs grown from these nanoparticles. The pore size of the block copolymer template in Figure 3a is 43 nm and the thickness of the deposited catalyst film is 7 nm. The catalyst size has been reduced from 43 to 34 nm after heat treatment. The CNTs grown from these catalysts have a diameter of about 16 nm and a wall thickness of about 5.2 nm, corresponding to the existence of 15–17 walls (Fig. 3b). High-resolution TEM images reveal that the CNTs have a bamboo-like structure because of the ammonia environment in the PECVD chamber.[24,25] Upon decreasing the pore size of the block copolymer template to 21 nm and the thickness of the deposited catalyst film to 7 nm (Fig. 3c and d), the catalyst nanoparticles have been found to be 16 nm in size after heat treatment. The CNTs grown from these catalysts have a diameter of 9 nm and a wall thickness of 2.5 nm, corresponding to the existence of 7–9 walls. The size of the catalyst nanoparticles and the CNT diameter can be further reduced by depositing a thinner catalyst film. Upon further decreasing the thickness of the deposited catalyst film to 3.5 nm for pores with a diameter of 21 nm (Fig. 3e and f), the obtained CNTs have a diameter of 6 nm, and the wall thickness is 1.4 nm, corresponding to the presence of 4–5 walls. The diameter and aerial density of vertically grown CNTs can be independently controlled by varying the molecular weight of the template material and the thickness of the catalyst film.

Figure 4 summarizes the statistical analysis results for the catalyst size and the diameter of the CNTs. As described above, the catalyst size is typically decreased after heat treatment and the final size of the catalyst is influenced by the pore size of the nanotemplate and the thickness of the deposited catalyst film. Figure 4b presents the statistical distribution of the CNT diameters obtained for the various catalyst nanoparticles. Both the CNT diameters and the thickness of the CNT walls are proportional to the diameter

ADVANCED MATERIALS

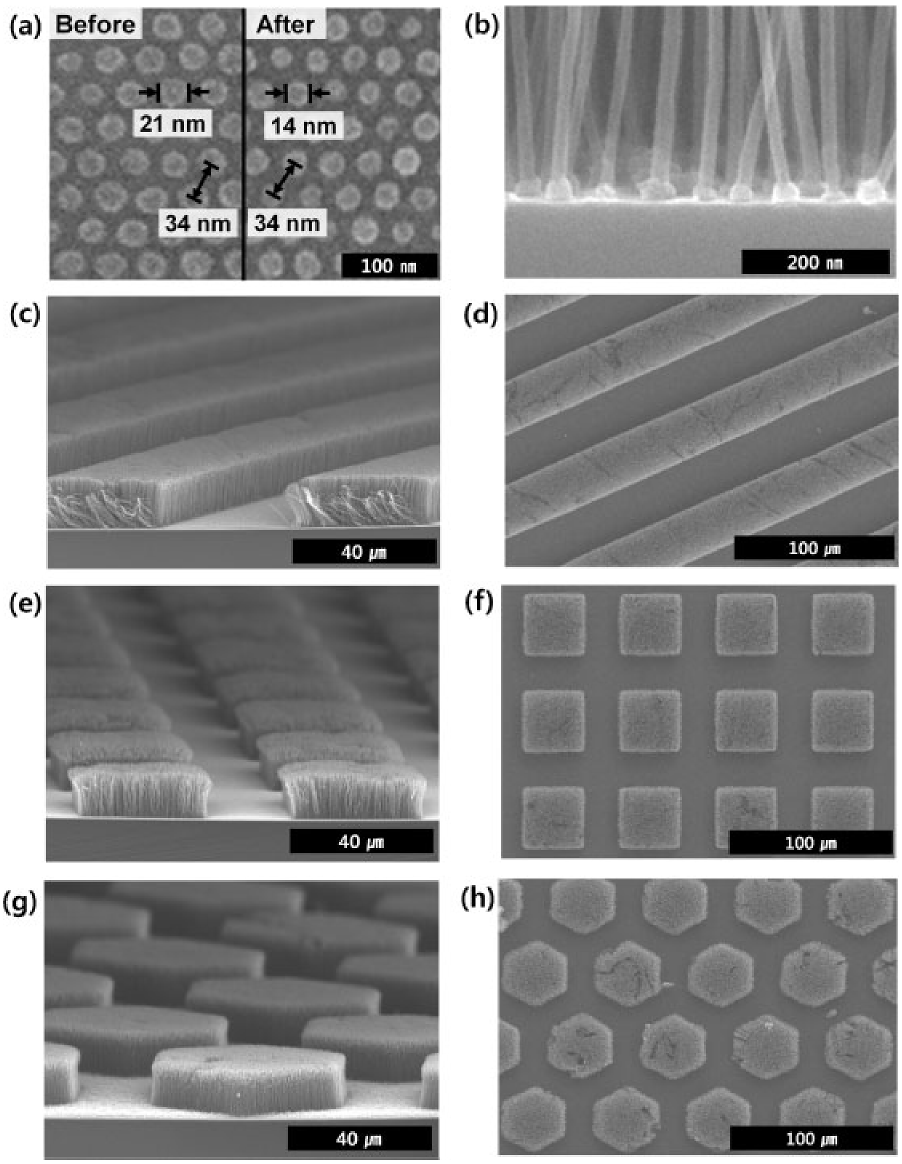

Figure 2. a) High-magnification scanning electron microscopy (SEM) image of nanopatterned iron catalyst particles before (left) and after (right) heat treatment. The hexagonal arrangement of the catalyst particles precisely duplicates the morphology of the nanotemplate. The average size of the particles is reduced from 21 to 14 nm after heat treatment. b) High-magnification cross-sectional SEM image of CNTs grown from catalyst nanoparticles. The diameter of the CNTs is approximately half of the catalyst particle size. c) Cross-sectional and d) plane-view SEM image of a hierarchical CNT array prepared using a parallel grid. e,f) SEM image of a hierarchical CNT array prepared using a square grid. g,h) SEM image of a hierarchical CNT array prepared using a hexagonal grid.

of the iron nanoparticles and the thickness of the deposited catalyst film.

The CNTs grown by a catalytic CVD method have been observed to be spontaneously oriented upwards because of the self-supporting influence of neighboring CNTs.[16] However, conventional thermal CVD does not yield a highly oriented vertical architecture because of the thermal fluctuations and gas flows established within the chamber during the growth process.[26] As the aspect ratio of the CNTs increases, the CNT alignment becomes successively poorer.[24,27] In order to enhance the vertical alignment, which is crucial for various applications in microelectronic devices, a PECVD method has been used. The electric field established in the PECVD chamber enhances the vertical alignment of the CNTs because of the high electrical polarizability of these structures. The large dipole moments induced in CNTs by the external electric field impose aligning torques on the growing CNTs, resulting in the growth of highly oriented vertical CNT arrays.[26,28,29]

In a capacitively-coupled plasma, a strong electric field can be focused along the narrow cathode sheath region (Fig. 5a).[30] The width of the cathode sheath region (d) can be estimated by the following equation:

$$d \propto \lambda_D = \left(\frac{\varepsilon_0 T_e}{e n_0}\right)^{1/2} \tag{2}$$

where λ_D is the Debye shielding length, n_0 is the electron density, ε_0 is the permeability of free space, and T_e is the electron temperature. High working pressures increase n_0 and reduce T_e, thus decreasing d.[31,32] In the present experiments, the distance between the two electrodes has been fixed at 1 cm and a dc voltage of 650 V has been applied to the anode relative to the grounded sample. For experiments using an ammonia environment, d has been estimated to be about 3 mm at 30 torr (1 torr = 133 Pa), whereas it is only 1 mm at 400 torr. The reduced sheath region enhances the electric field in the sheath region. Figure 5b and c shows high-resolution SEM images demonstrating the influence of the chamber pressure on the degree of vertical alignment of CNTs. The alignment of CNTs is poor at a working pressure of 30 torr. In contrast, the CNTs are highly aligned at a pressure of 400 torr. The diameter of the CNTs remains the same and is not influenced by varying the working pressure inside the chamber.

In conclusion, we have demonstrated a facile and robust hierarchical organization process for obtaining vertically aligned CNT arrays. The masked deposition of a catalyst over a nanoporous block copolymer film provides control over the size and large-area lateral ordering of catalyst particles on

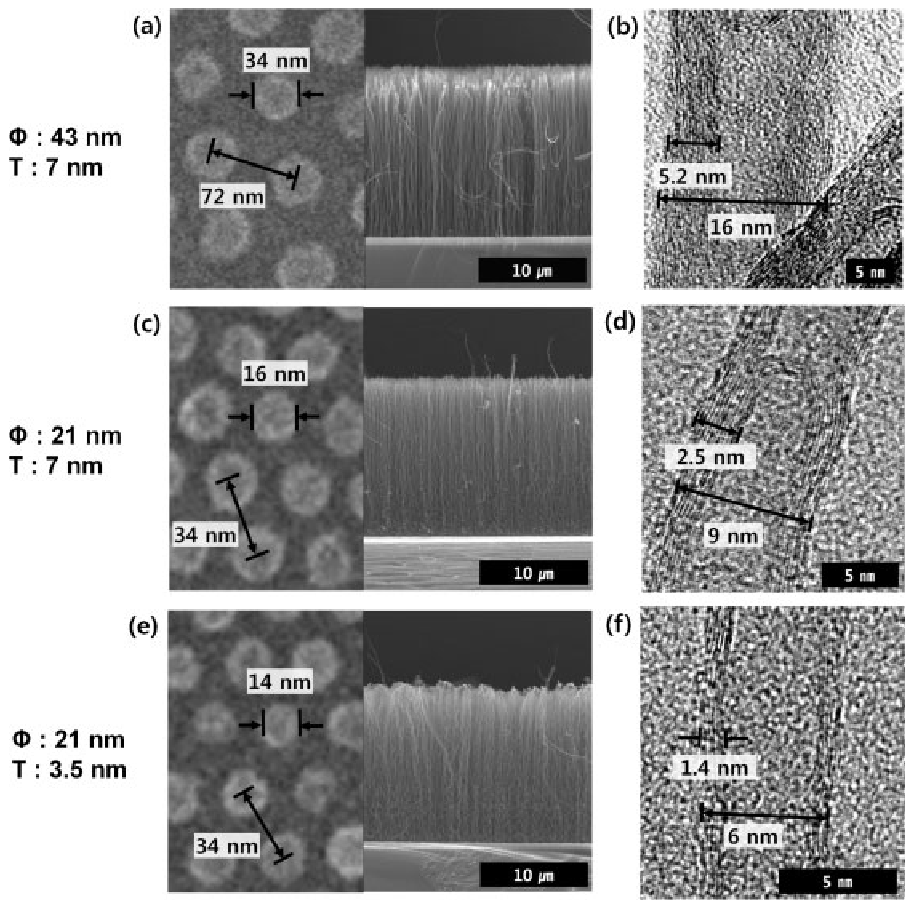

Figure 3. Plots of the nanopore size in the block copolymer nanotemplate (Φ) and the thickness of the iron catalyst (T) versus the diameter and wall thickness of the obtained CNTs. Upon tuning Φ and T for the deposited catalyst, the average diameter and aerial density of the CNTs can be independently controlled. SEM images of nanopatterned catalyst particles and the corresponding vertical CNTs along with high-resolution TEM images of the CNTs for a,b) $\Phi = 43$ nm and $T = 7$ nm; c,d) $\Phi = 21$ nm, $T = 7$ nm; and e,f) $\Phi = 21$ nm, $T = 3.5$ nm.

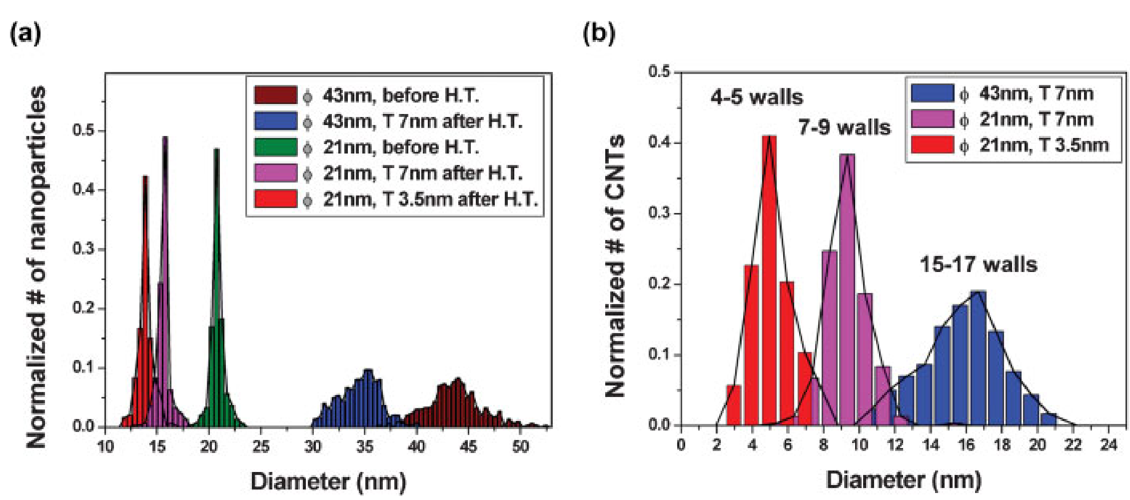

Figure 4. Statistical size distribution of a) catalyst nanoparticles before and after heat treatment and b) CNTs grown from the catalyst nanoparticles. Both the diameter and the wall thickness of the CNTs are proportional to the catalyst size.

ADVANCED MATERIALS

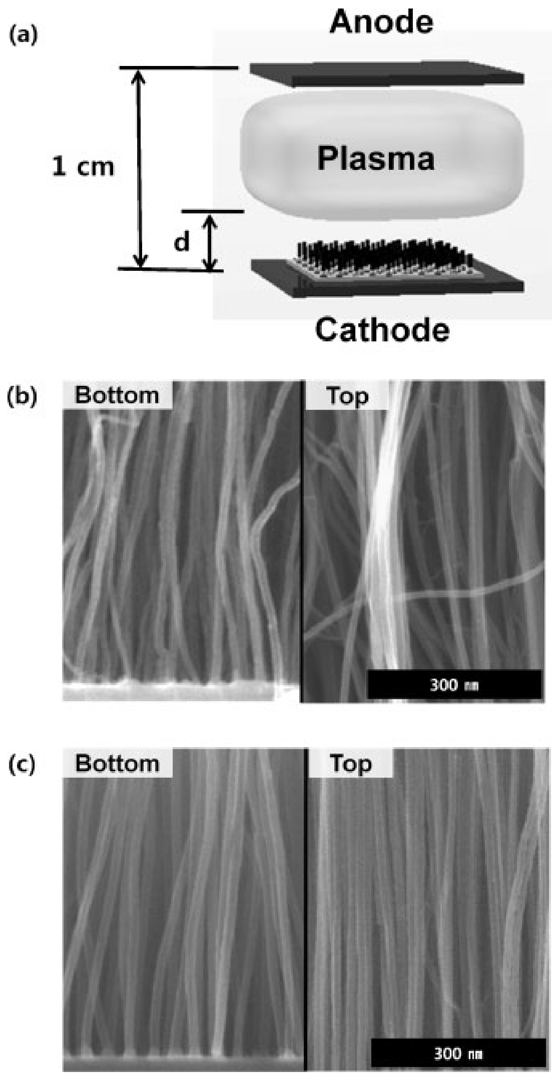

Figure 5. a) Schematic depiction of the PECVD growth of a vertical CNT array. The vertical distribution of the plasma determines the width of the cathode sheath region (d). High-magnification SEM images of the bottom and top parts of vertical CNTs grown at chamber pressures of b) 30 torr and c) 400 torr. The chamber pressure of 400 torr provides an electric field strong enough to produce highly aligned CNTs.

the substrate. The PECVD growth of CNTs from laterally patterned catalyst arrays yields highly oriented vertical CNTs; the CNTs are uniform in diameter and the lateral distribution of the CNTs is hierarchically ordered and follows the distribution of the catalyst particles. In this novel approach, the morphology of individual CNTs and the 3D organization of CNTs are both independently tunable. In other words, parameters such as the CNT diameter, local and large-area lateral distributions, and the degree of vertical alignment can all be separately adjusted. Furthermore, this approach may potentially be useful for the catalytic growth of other 1D nanomaterials, suggesting interesting possibilities for the device integration of various functional nanomaterials.

Experimental

Materials: Asymmetric block copolymers, PS-*b*-PMMA forming cylindrical nanostructures (molecular weights, PS/PMMA of 140 k/60 k, D for PMMA = 43 nm, L = 72 nm; and molecular weights, PS/PMMA of 46k/21k, D for PMMA = 21 nm, L = 34 nm) were purchased from Polymer Source. The iron source for electron-beam evaporation (purity: 99.95%) was purchased from Thifine. Pure ammonia and acetylene gases were purchased from Showa Denko K.K. and Kyungin Chemical Industrial, respectively. Copper grids for TEM analysis were purchased from Electron Microscopy Sciences.

Preparation of Nanopatterned Catalyst Particles: The surface of a silicon wafer was treated with a random brush copolymer, and a thin film (thickness: 60 nm) of the block copolymer was spin-coated onto the wafer surface. After high-temperature annealing at 190 °C, the substrates were irradiated with UV light and subsequently rinsed with acetic acid and water to remove the PMMA cylinder cores and crosslink the PS matrix. The substrate was then treated with oxygen plasma for 10 s in order to remove the remnant cylinder cores. Subsequently, an iron catalyst film was deposited over a selective region of the block copolymer. Copper grids with various shapes were used as masks in the selective deposition step. After the deposition process, the remnant PS nanoporous template was lifted-off by ultrasonication in toluene. This process yielded catalyst nanoparticles of uniform size, arrayed along the hexagonal nanotemplate lattice at predefined areas.

PECVD Growth of Vertical CNTs: CNT growth was carried out on the catalyst-deposited substrates using PECVD. The substrate was first heated to 750 °C under a 100 sccm flow of ammonia gas (chamber pressure: 1.3 torr). After the substrate temperature reached 750 °C, the substrate was thermally annealed (typically for less than 3 min) in order to reduce the size of the catalyst particles. The chamber pressure was then increased to 400 torr and the dc plasma was activated using an anode dc voltage of 650 V relative to the grounded substrate. After the introduction of acetylene gas at a flow rate of 25 sccm for 1 min, the substrate was covered with a dense multiwalled CNT array grown from the catalyst array. The growth rate of the CNT arrays was approximately 16.3 μm min^{-1}.

Received: November 1, 2007
Published online: November 15, 2007

[1] H. Dai, E. W. Wong, C. M. Lieber, *Science* **1996**, *272*, 523.
[2] P. M. Ajayan, T. W. Ebbesen, *Rep. Prog. Phys.* **1997**, *60*, 1025.
[3] S. J. Kang, C. Kocabas, T. Ozel, M. Shim, N. Pimparkar, M. A. Alam, S. V. Rotkin, J. A. Rogers, *Nat. Nanotechnol.* **2007**, *2*, 230.
[4] B. Q. Wei, R. Vajtai, Y. Jung, J. Ward, R. Zhang, G. Ramanath, P. M. Ajayan, *Nature* **2002**, *416*, 495.
[5] Y. J. Jung, B. Wei, R. Vajtai, P. M. Ajayan, Y. Homma, K. Prabhakaran, T. Ogino, *Nano Lett.* **2003**, *3*, 561.
[6] W. A. DeHeer, A. Chatelain, D. Ugarte, *Science* **1995**, *270*, 1179.
[7] S. J. Tans, A. R. M. Verschueren, C. Dekker, *Nature* **1998**, *393*, 49.
[8] L. Delzeit, C. V. Nguyen, B. Chen, R. Stevens, A. Cassell, J. Han, M. Meyyappan, *J. Phys. Chem. B* **2002**, *106*, 5629.
[9] A. J. Hart, A. H. Slocum, L. Royer, *Carbon* **2006**, *44*, 348.
[10] R. G. Lacerda, K. B. K. Teo, A. S. The, M. H. Yang, S. H. Dalal, D. A. Jefferson, J. H. Durell, N. L. Rupesinghe, D. Roy, G. A. J. Amaratunga, W. I. Milne, F. Wyczisk, P. Legagneux, M. Chhowalla, *J. Appl. Phys.* **2004**, *96*, 4456.
[11] S. Hofmann, M. Cantoro, B. Kleinsorge, C. Casiraghi, A. Parvez, J. Robertson, C. Ducati, *J. Appl. Phys.* **2005**, *98*, 034308.
[12] D. N. Futaba, K. Hata, T. Namai, T. Yamada, K. Mizuno, Y. Hayamizu, M. Yumura, S. Iijima, *J. Phys. Chem. B* **2006**, *110*, 8035.

[13] M. Park, C. Harrison, P. M. Chaikin, R. A. Register, D. H. Adamson, *Science* **1997**, *276*, 1401.
[14] T. Thurn-Albrecht, J. Schotter, G. A. Kastle, N. Emley, T. Shibauchi, L. Kruxin-Elbaum, K. Gaurini, C. T. Black, M. T. Touminen, T. P. Russell, *Science* **2000**, *290*, 2126.
[15] J. Y. Cheng, C. A. Ross, H. I. Smith, E. L. Thomas, *Adv. Mater.* **2006**, *18*, 2505.
[16] R. D. Bennett, A. J. Hart, R. E. Cohen, *Adv. Mater.* **2006**, *18*, 2274.
[17] J. Li, K. Kamata, S. Watanabe, T. Iyoda, *Adv. Mater.* **2007**, *19*, 1267.
[18] S. O. Kim, H. H. Solak, M. P. Stoykovich, N. J. Ferrier, J. J. dePablo, P. F. Nealey, *Nature* **2003**, *424*, 411.
[19] M. P. Stoykovich, M. Muller, S. O. Kim, H. H. Solak, E. W. Edwards, J. J. de Pablo, P. F. Nealey, *Science* **2005**, *308*, 1442.
[20] S. O. Kim, B. H. Kim, K. Kim, C. M. Koo, M. P. Stoykovich, P. F. Nealey, H. H. Solak, *Macromolecules* **2006**, *39*, 5466.
[21] S. O. Kim, B. H. Kim, D. Meng, D. O. Shin, C. M. Koo, H. H. Solak, Q. Wang, *Adv. Mater.* **2007**, *19*, 3271.
[22] P. Mansky, Y. Liu, E. Huang, T. P. Russell, C. Hawker, *Science* **1997**, *275*, 1458.
[23] D. Y. Ryu, K. Shin, E. Drockenmuller, C. J. Hawker, T. P. Russell, *Science* **2005**, *308*, 236.
[24] M. J. Jung, K. Y. Eun, Y. J. Baik, K. R. Lee, J. K. Shin, S. T. Kim, *Thin Solid Films* **2001**, *398–399*, 150.
[25] M. Lin, J. P. Y. Tan, C. Boothroyd, K. P. Loh, E. S. Tok, Y. L. Foo, *Nano Lett.* **2007**, *7*, 2234.
[26] Y. Zhang, A. Chang, J. Cao, Q. Wang, W. Kim, Y. Li, N. Morris, E. Yenilmez, J. Kong, H. Dai, *Appl. Phys. Lett.* **2001**, *79*, 3155.
[27] Y. Y. Wei, G. Eres, V. I. Merkulov, D. H. Lowndes, *Appl. Phys. Lett.* **2001**, *78*, 1394.
[28] A. Nojeh, A. Ural, R. F. Pease, H. Dai, *J. Vac. Sci. Technol. B* **2004**, *22*, 3421.
[29] J. F. AuBuchon, L. H. Chen, A. I. Gapin, D. W. Kim, C. Daraio, S. H. Jin, *Nano Lett.* **2004**, *4*, 1781.
[30] T. Kato, R. Hatakeyama, *Chem. Vap. Deposition* **2006**, *12*, 345.
[31] M. A. Liebermann, A. J. Lichtenberg, *Principles of Plasma Discharges and Materials Processing*, Wiley, New York **1994**, p. 450.
[32] Q. Yang, C. Xiao, W. Chen, A. K. Singh, T. Asai, A. Hirose, *Diamond Relat. Mater.* **2003**, *12*, 1482.